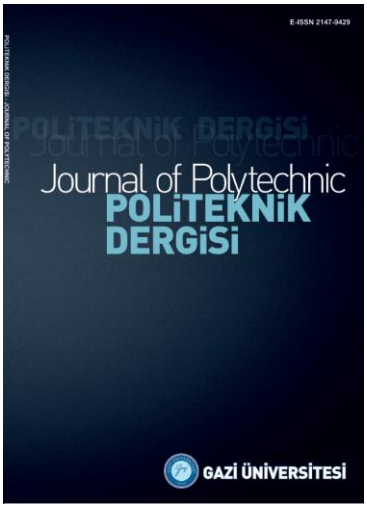

POLİTEKNİK DERGİSİ

JOURNAL of POLYTECHNIC

ISSN: 1302-0900 (PRINT), ISSN: 2147-9429 (ONLINE)
URL: http://dergipark.org.tr/politeknik

The effect of incorporating vertical spatial variability on the probabilistic analysis of a deep excavation: a case study

Derin kazıların olasılıksal analizi üzerinde düşey konumsal değişkenliğin etkisi: bir vaka çalışması

***Yazar(lar) (Author(s))**: Dursun Enes KORKUT[1], Sami Oğuzhan AKBAŞ[2]*

ORCID[1]: 0009-0009-1244-3961

ORCID[2]: 0000-0002-7872-1604

To cite to this article: Korkut D.E., Akbaş S.O., "The effect of incorporating vertical spatial variability on the probabilistic analysis of a deep excavation: a case study", ***Journal of Polytechnic***, 26(3): 1233-1242, (2023).

Bu makaleye şu şekilde atıfta bulunabilirsiniz: Korkut D.E., Akbaş S.O., "The effect of incorporating vertical spatial variability on the probabilistic analysis of a deep excavation: a case study", ***Politeknik Dergisi***, 26(3): 1233-1242, (2023).

Erişim linki (To link to this article): http://dergipark.org.tr/politeknik/archive

DOI: 10.2339/politeknik.1324358

The Effect of Incorporating Vertical Spatial Variability on the Probabilistic Analysis of a Deep Excavation: A Case Study

Highlights

- *One-dimensional random finite element method*
- *Impact of the scale of fluctuation on lateral wall displacements and maximum bending moments*
- *Comparisition against field measurements and deterministic solution.*

Graphical Abstract

This paper focuses on the effects of different scale of fluctuations on lateral wall displacements and maximum bending moments.

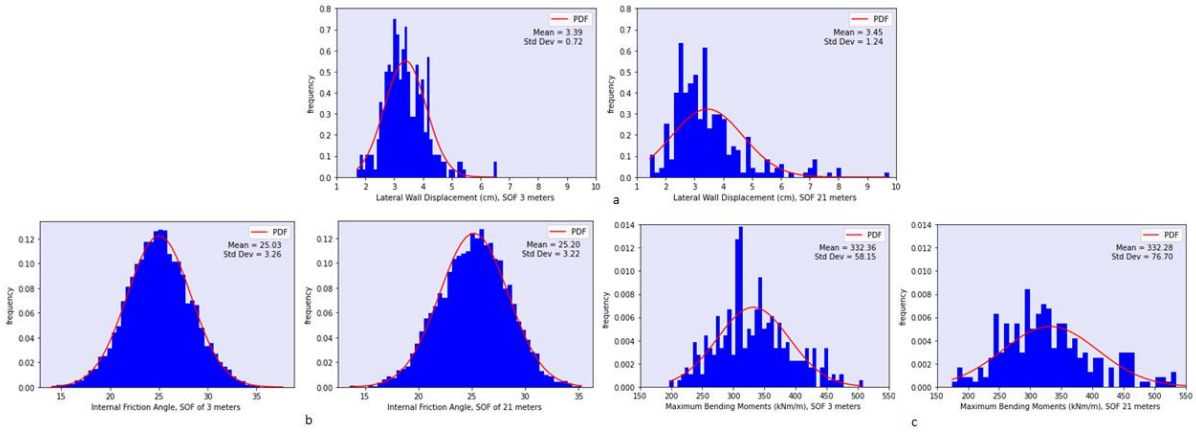

Figure. *Results of a)Lateral Wall Displacement, b)Effective Stress Friction Angles, c)Maximum Bending Moments*

Aim

In this study, the effects of scale of fluctuation on a random field are thoroughly examined and compared with real-life measurements. The primary objective is to investigate how variations in the scale of fluctuation influence the behavior of the random field and to compare these findings with the outcomes obtained through real-life measurements and deterministic modeling approaches.

Design & Methodology

Random finite element method employed to generate the effective stress friction angles with different scales of fluctuations while a lognormal distribution was utilized for the soil cohesion.

Originality

The effects of different scale of fluctuations on lateral wall displacements and maximum bending moments, and their comparisition against field measurements and deterministic solution.

Findings

A total of 6300 internal friction angles were generated for each scale of fluctuation. For each scale of fluctuation, 300 solutions were created. The results indicate that the scale of fluctuation of 3 meters has a failure percentage of 3%, while the scale of fluctuation of 21 meters has a failure percentage of 5.3%.

Conclusion

The scale of fluctuation of 3 meters yields better outcomes in terms of data distribution. On the other hand, the scale of fluctuation of 21 meters exhibits a larger range of data and tends to produce a significant number of overestimated values.

Declaration of Ethical Standards

The author(s) of this article declare that the materials and methods used in this study do not require ethical committee permission and/or legal-special permission.

Derin Kazıların Olasılıksal Analizi Üzerinde Düşey Konumsal Değişkenliğin Etkisi: Bir Vaka Çalışması

Araştırma Makalesi / Research Article

Dursun Enes KORKUT[1,2*], Sami Oğuzhan AKBAŞ[2]

[1]Milli Savunma Üniversitesi, Kara Harp Okulu, İnşaat Mühendisliği Bölümü, Türkiye
[2]Gazi Üniversitesi, Mühendislik Fakültesi, İnşaat Mühendisliği Bölümü, Türkiye

(Geliş/Received : 07.07.2023 ; Kabul/Accepted : 26.07.2023 ; Erken Görünüm/Early View : 17.08.2023)

ÖZ

Bu çalışmada, derin kazıların olasılıksal analizinde kilin efektif içsel sürtünme açısının düşey konumsal değişkenliğinin dahil edilmesinin etkisi araştırılmaktadır. Önerilen metodoloji, Türkiye'nin Ankara ilinde bulunan enstrümantasyonlu bir derin kazı projesinin rastgele sonlu eleman modellemesi (RFEM) kullanılarak örneklendirilmiş ve doğrulanmıştır. Kazı, 20 metre derinliğe sahiptir ve altı seviyede öngermeli zemin ankrajları ile desteklenmektedir. Kilin efektif içsel sürtünme açısının düşey konumsal değişkenliğini benzeştirmek için rastgele alan teorisi ve Monte Carlo simülasyonu kullanılmıştır. Benzeştirme ile üretilen parametreler daha sonra Python yazılım dili aracılığıyla sonlu eleman modeline yerleştirilerek, fore kazık iksa yapısında yanal deformasyonlar ve eğilme momentlerinin olasılıksal dağılımı incelenmiştir. Monte Carlo simülasyonlarından elde edilen sonuçlar, konumsal değişkenliğin göz önünde bulundurulmasının ve değerinin ortaya çıkan yanal deformasyonlar, eğilme momentleri ve sistem yenilme olasılığı üzerinde etkisinin olduğunu göstermektedir.

Anahtar Kelimeler: Monte carlo simülasyonu, rasgele alan teorisi, sonlu elemanlar yöntemi.

The Effect of Incorporating Vertical Spatial Variability on the Probabilistic Analysis of a Deep Excavation: A Case Study

ABSTRACT

This study explores the impact of including the vertical spatial variability in effective stress friction angle of clay on the probabilistic analysis of deep excavations. The proposed methodology is demonstrated and verified by conducting random finite element modeling (RFEM) of an instrumented deep excavation project situated in Ankara, Turkey. The excavation has a depth of 20 meters and is supported by six levels of pre-stressed ground anchors. To simulate the vertical spatial variability of effective stress friction angle in the clay, Monte Carlo simulation method and the random field theory are employed. The simulated parameters are then inserted into the finite element model via Python programming language to analyze the probabilistic distribution of lateral deflections and bending moments in the drilled shaft wall. The results obtained from the Monte Carlo simulations reveal that the incorporation and selected value of spatial variability significantly impacts the resulting lateral movements, bending moments, and the probability of failure of the system.

Keywords: Monte carlo simulation, random field theory, finite element method.

1. INTRODUCTION

In contrast to fields like mechanical or structural engineering where materials typically have relatively homogeneous properties, geotechnical engineering faces the difficulty of estimating and quantifying the in-situ soil and rock parameters. Soil exhibits substantial variability, and even small distances can result in significant variations in its properties. Moreover, site investigations in geotechnical engineering are both limited in extent and prone to errors, further adding to the challenge of accurately characterizing the ground conditions.

A multitude of challenges can emerge from site investigation to laboratory testing, giving rise to These uncertainties can be placed under three primary sources [1]: Transformation uncertainties, measurement error, and inherent soil variability. The presence of transformation uncertainties arises when field and laboratory measurements are translated into design soil properties through the application of empirical correlation models. Measurement errors in geotechnical testing can arise from various sources, including equipment limitations, procedural errors, and random testing effects. Inherent soil variability refers to the natural variation in soil parameters between different spatial locations within a soil mass [2]. The presence of these three errors can significantly impact the accuracy and reliability of the obtained data. The combination of these factors collectively introduces significant amount of uncertainties into the analysis and design processes, affecting the reliability and accuracy of the outcomes. Deterministic analysis methods are useful tools, but their reliability is contingent upon having enough and accurate information about the site. When such information is

*Sorumlu yazar (Corresponding Author)
e-posta : korkutdursunenes@gmail.com

lacking, the results they produce may overestimate or underestimate the performance observed in the field. In situations where sufficient data is not available, a different approach needs to be adopted.

This innovative approach to address the problem is the utilization of probabilistic methods, where uncertainty-based modelling of random parameters can be made based on the extent of data acquired for the project as well as on previously published values [3]. The probabilistic or reliability-based analyses in geotechnical engineering are a necessity due to the spatial variability of soil, limited models, limited site exploration and uncertainties in soil parameters [4]. The imprecise nature of geotechnical engineering necessitates the adoption of a probabilistic approach which is essential for achieving a comprehensive understanding of potential outcomes and making informed decisions in the field.

To this end, recently, the advancements in computational tools have also facilitated the analysis of deep excavations using probabilistic numerical approaches. However, the influence of soil spatial variability has been extensively studied in various geotechnical design scenarios involving slopes, gravity retaining walls, tunnels and shallow foundations [5-11]. Despite this, there are insufficient amount of studies focusing on the impact of spatial variation, particularly in relation to probabilistic analysis of deep excavations.

Sert et al. [12] conducted a study on the impact of vertical spatial variability of soil properties for excavations supported by cantilever walls in sand. Luo et al. [13] investigated multiple structural and geotechnical failure modes, considering the influence of vertical spatial variability on supported excavations in sand. However, it is important to highlight that these mentioned studies that explore the contribution of spatial variability of cohesionless soils have only utilized hypothetical design examples, with a limited number of research based on actual case studies.

The only exception is the recent study by Nguyen and Likitlersuang [14], which presents a two-dimensional RFEM analysis considering the unpredictability of undrained shear strength for the reliability analysis of a deep excavation in Bangkok that utilized reinforced concrete diaphragm walls. This study focuses on a specific scale of fluctuation (SOF) value for clay layers and does not account for any variations in the SOF. As a result, the study's findings do not reflect the potential impact that changes in the SOF can have on the results. Currently, there is not enough studies that specifically investigate the impact of various values of spatial variability of drained soil parameters in clay on the performance of excavation support systems using verified modelling through actual deformation measurements.

Based on these considerations, in this study, the focus is on investigating the effective stress friction angle' vertical spatial variability, and its impact on wall displacement. To achieve this, a one-dimensional random field is created using a set of five steps. Firstly, a sequence of independent standard normal random variables is generated. Then, a correlation structure is established to capture the spatial dependency between these variables. The Cholesky decomposition technique is employed to construct the covariance matrix. Subsequently, a correlated standard normal random field is generated by applying the Cholesky decomposition to the independent random variables. Finally, the mean and variance are reintroduced to the independent random field to align it with the desired statistical properties. After the validation of the finite element method (FEM) model by comparing the model results with field observations, i.e., inclinometer readings, multiple FEM models are then created by mapping the series of generated spatial variability using Python interface [14]. The findings are analyzed and discussed to offer valuable insights into how spatial variability influences the lateral wall movements in a deep excavation supported by drilled shafts and prestressed anchors in clay.

2. MATERIAL and METHOD

2.1. Case Study and Finite Element Method

A deep excavation for a hotel construction located in Ankara, Turkey is considered. Overlaid by a 3 m thick fill, the predominant soil composition in the area is clay, with occasional bands of gravelly sand. The 20 m-deep excavation's support system consists of 21 m long, 65 cm diameter drilled shafts with six levels of pre-stressed anchors with fixed lengths of 7 m, each inclined at an angle of 15°, and spaced at a distance of 2.5 m and 3 m, in vertical and horizontal, respectively. A photograph of the completed excavation can be seen in Figure 1 [16].

Figure 1. A View of the Investigated Drilled Shaft Wall (Çalışan, 2009).

The finite element analyses of the excavation were conducted using PLAXIS 2D program [17]. This software offers an automated parameter mapping feature for Monte Carlo simulations and includes a Python interface for enhanced functionality. Utilizing PLAXIS 2D, it becomes possible to determine failure mechanisms when wall lateral displacement limits and drilled shaft lateral capacities are exceeded. Figure 2 depicts the FEM geometry, which represents the structural elements and idealized soil layers of the excavation, incorporating the specific parameters and dimensions of the site. It is important to note that for the convenience of assigning input soil parameters in the RFEM, the upper clay layer

has been divided into 21 horizontal layers, each with a thickness of 1 meter. This division allows for a more straightforward and efficient process of parameter assignment in the RFEM analyses.

In order to mitigate the boundary effects on wall displacements, specific boundary conditions have been applied in this study. The boundary conditions have been set as follows: The left-side boundary is fixed at a distance of 42 meters from the pile wall. In all scenarios, the lower boundary is consistently positioned 80 meters below the ground surface. The bottom boundary is subject to constraints in both vertical and horizontal movements, while the right and left-side boundaries are solely restricted horizontally, in accordance with standard practice. These boundary conditions have been determined in accordance with previous studies on boundary specifications for excavation models, as emphasized by Brinkgreve [18].

The soil mass is simulated using 15-node triangular soil elements, while the drilled shaftwall is modeled using 5-node plate elements. The finite element model includes 5839 soil elements and 47207 nodes, with 47 plate elements representing the drilled shaft wall.

The stress-strain response of clay is replicated through the utilization of the hardening soil (HS) constitutive relationship. The HS model, a widely employed nonlinear constitutive model in soil simulations, is used to simulate soil behavior. Within this model, failure is determined by the Mohr-Coulomb (MC) failure criterion. By incorporating a hyperbolic correlation between axial strain and deviatoric stress, the HS model exhibits a distinctive characteristic [19]. The HS model is particularly effective in unloading conditions such as excavations, providing more reliable displacement predictions compared to the MC model. Çalışan (2009) performed inverse analyses based on the obtained inclinometer readings from the excavation to identify the HS model geotechnical parameters for the finite element modelling of clay, with results summarized in Table 1. As depicted in Figure 3, the maximum lateral wall displacement was measured to be 2.6 cm.

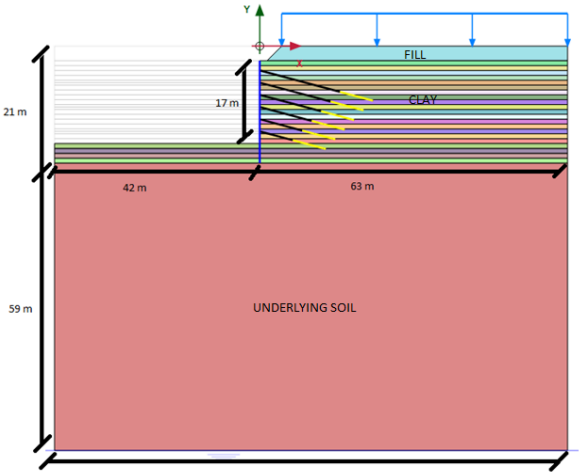

Figure 2. The FEM Geometry

In this study, the soil parameters obtained by Çalışan (2009) are adopted as mean values. Table 1 summarizes the mean geotechnical parameters assigned to the clay layer for the FEM analyses.

By conducting a deterministic finite element analysis using the mean parameters given in Table 1, the lateral displacement and maximum bending moment in the wall were determined to be 2.6 cm and 236 kN.m/m respectively. The calculated displacement values exhibits agreement with the inclinometer measurements. This correspondence between the model results and the actual behavior observed in the field indicates that the finite element model realistically simulates the behavior of the excavation support system with the assigned geotechnical properties. Note that as the installation procedure and exact coordinates of the inclinometers were not accessible, the authors relied only on the

Table 1. Mean Parameters for the Clay Layers

Parameters	**Fill**	**Clay**	**Underlying Soil**	**Unit**
Material Model	Hardening Soil	Hardening Soil	Hardening Soil	-
Drainage Type	Drained	Drained	Drained	-
E_{50}^{ref}	12000	55000	110000	kN/m^2
E_{oed}^{ref}	12000	55000	110000	kN/m^2
E_{ur}^{ref}	36000	165000	330000	kN/m^2
Power (m)	0.5	0.5	0.5	-
Effective cohesion	3	20	25	kN/m^2
Effective Stress Friction Angle, ϕ' (°)	25	25	25	°
R_{inter}	0.7	0.7	0.8	-
Undrained Shear Strength, (s_u)	-	200	-	kN/m^2

maximum magnitude recorded from the available inclinometer data for comparisons.

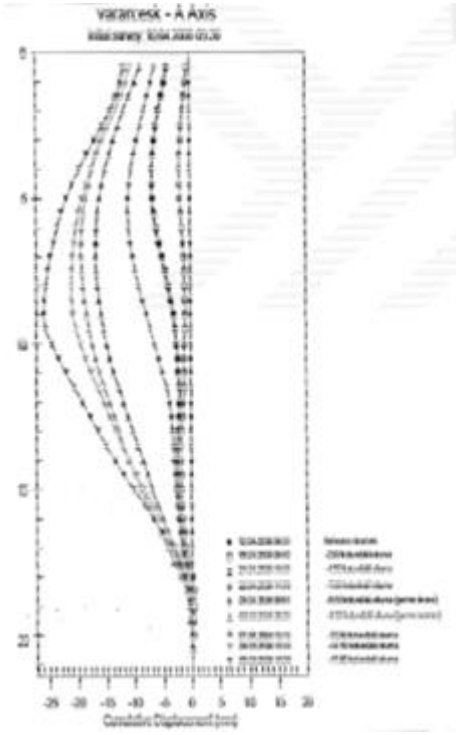

Figure 3. Inclinometer Results (Çalışan, 2009)

2.2. Uncertainty Modelling

In this study, the selected values of the drained cohesion of the soil, which is not very influential on the displacements, and the pre-stressing value of anchors that was measured in the field loading tests were not modified from previous studies [20]. However, a random field was generated specifically for the effective stress friction angle of the clay layer, which in turn effects the drained modulus. This section presents the chosen statistical parameters for characterizing the random field of the effective stress friction angle.

In order to accurately capture the variability of soil properties, it is essential to determine the mean and COV values for the most influential geotechnical parameters. The mean values for the parameters were presented in Table 1. Phoon and Ching [21] conducted a comprehensive study on the COV of clays, and their collected data regarding the COV is presented in Table 2. This dataset provides valuable information for understanding the variability of clay soils and can be used for further analysis and comparison in this study. Additionally, Akbas and Kulhawy [22] specifically investigated the variability of the properties of Ankara Clay. Table 3 presents the findings from their research. Based on these information, the COV value of undrained soil strength and the effective stress friction angle were selected as 23% and 13%, respectively.

To calculate the drained cohesion (c') from the undrained shear strength, the equation proposed by Sorensen and Okkels [23] was employed:

$$c' = s_u \times 0{,}1 \quad (1)$$

In the course of the analyses, particular attention was given to water-bearing sand-gravel bands that are frequently encountered in the Ankara Clay. The objective was to examine the detrimental impact of these bands on the behavior of the excavation system. Previous research [20] highlights that these bands lead to a significant reduction in anchor capacity, with failure loads from anchor tests ranging between 70-200 kN. Remarkably, these values are significantly lower than half of the typical lateral wall displacement typically observed in the Ankara Clay. Thus, considering the presence of these water-bearing sand-gravel bands is crucial when assessing the performance of the excavation system.

Based on extensive site investigations and laboratory tests conducted in the Akyurt and Kazan regions of Ankara, it was determined that the thickness of the sand-gravel layers within the Ankara Clay sums up to be approximately 15% of the total depth of the boreholes for the first 20 m depth [24]. In order to account for the possible existence of sand-gravel bands within the fixed length of the anchor, the prestress value of the anchors was adjusted in the finite element (FEM) calculations. To achieve this, a Python code was prepared to randomly select the prestress value, considering a uniform weight distribution of 85% for the clay layer and 15% for the sand-gravel layer. Specifically, the anchors were prestressed with 400 kN for the clay layer, while for the sand-gravel layer, a prestress value ranging from 70-200 kN was randomly chosen using Python, with equal probability weights as summarized in Table 4. This approach, in a conservative way, allowed for a comprehensive assessment of the anchor prestress, taking into account the variability introduced by the presence of the sand-gravel layer.

2.3. Generation of Random Field

As mentioned before soil is a spatially variable material, and its parameters can change significantly within small distances. However, it is important to note that while these parameters exhibit spatial variability, they are not completely random. One prominent feature of random field representation is the concept of dependence between soil parameters at different points. Random field theory is a powerful tool for modeling spatial variations and interdependence that cannot be adequately captured by deterministic methods or conventional statistics [25].

Table 2. Coefficient of Variables (COV) Values of Soil Parameters from Literature (Phoon and Ching, 2015)

Parameter	COV (%)
Undrained Shear Strength (s_u)	13-40
Effective Stress Friction Angle (ϕ')	2-13

Table 3. Mean Parameters and Their Variabilities of Ankara Clay (Akbas and Kulhawy, 2010)

Parameters	Number of Data Groups	Number of Test for Each Group	Parameter value		Parameter COV_w (%)	
			Range	Mean	Range	Mean
W (%)	25	4-24	50-79	64	9-22	14
W_p (%)	25	4-25	20-35	26	6-19	12
W_n (%)	26	4-18	23-37	29	12-22	4
PI (%)	25	4-24	21-52	38	13-28	19
e_o	14	4-25	0.65-0.98	0.84	3-16	9
γ_d (kN/m³)	20	3-12	14-17	15.8	2-8	5
s_u (kN/m²)	9	4-8	106-186	148	11-35	23
C_c	7	3-8	0.18-0.38	0.26	14-35	26
SPT N	12	6-31	23-60	38	10-46	29

Table 4. Anchor Prestresses According to the Soil Layers

Soil	Anchor Prestress (kN)	Probability (%)
Clay	400	85
Sand-Gravel Layer	70-200 (Uniform distribution)	15

It is noteworthy to mention that in this study, the variability of the clay layer was only considered for the first 21 m thickness, which encompasses the majority of the excavation area, it accounts for entire fixed lengths of the ground anchors. It should be acknowledged that the clay layer below this depth may only have a slight impact on the lateral displacement profile since the clay is stiff-hard, and therefore no potential for bottom heave exists.

To facilitate the specification of input soil parameters in the RFEM, the upper clay layer has been divided into 21 horizontal layers, each with a thickness of 1 m. For the random field, the internal friction angle is normally distributed with a mean of 25º and COV of %13.

Once these decisions are made, the next step is to select the SOF refers to the maximum correlation distance for the spatially random parameters. The SOF is a crucial parameter as it influences the range and variability of the random field. A smaller SOF signifies a higher level of spatial variability, meaning that the properties of the field exhibit more pronounced fluctuations over smaller distances. As the size of the SOF approaches zero, the random field transitions into a stochastic state, resulting in uncorrelated elements within the field. Conversely, a larger SOF value indicates a reduced level of spatial variability. When the SOF tends towards infinity, the random field becomes spatially constant, indicating that the field properties remain relatively uniform over greater distances.

According to Akbas and Kulhawy [22], the vertical SOF for Ankara Clay is reported as 2.0 m and 3.4 m for s_u and SPT N values, respectively. Based on this limited information, a value of 3 m is chosen as the vertical SOF for the effective stress friction angle in this study. Additionally, for comparison and illustration purposes, a much larger vertical SOF of 21 m, which represents the entire thickness of the clay layer, is also considered.

It is noteworthy that in geotechnical engineering problems, the horizontal SOF generally exhibits larger values, and its influence is relatively less significant when compared to the vertical SOF. Therefore, in this study, the focus is primarily on the vertical spatial variability of the effective stress friction angle, as it has a much greater influence on the behavior of the excavation system.

A five-step process is employed to generate random fields, based on [26]:

1. Initially, a sequence of independent standard normal random variables is generated. These variables serve as the basis for generating the random field. To generate standard normal variates, random variables that are uniformly distributed between 0 and 1, such as U_i and U_{i+1}, can be utilized. An example of this process is given by:

$$Z_i = \sqrt{-2\ln(1-U_i)}\cos(2\pi U_{i+1}) \quad (2)$$

$$Z_{i+1} = \sqrt{-2\ln(1-U_i)}\sin(2\pi U_{i+1}) \quad (3)$$

2. To account for the interdependence between variables, a correlation matrix must be created. The correlation structure is commonly perceived as a function of the spatial distance between points. The exponential decay model [26] is widely adopted to represent the correlation between points, where the degree of correlation decreases as the distance between points increases:

$$p(\tau) = \exp((\frac{-2\tau}{\theta}) \quad (4)$$

In the equation 4 , τ symbolizes the distance between the centers of two layers, and Θ signifies the SOF. Figure 4 presents a correlation matrix sized 21 x 21 generated by Python for a SOF of 3 meters.

Figure 4. Correlation Matrix for SOF of 3 Meters

3. Cholesky decomposition is performed, which allows for the transformation of the independent standard normal variables into correlated standard normal variables:

$$LL^T = p \quad (5)$$

4. Using the Cholesky decomposition results, a correlated standard normal random field is created. This field represents the spatial variability of the studied parameter. By performing a linear combination of independent standard normal variates, a properly correlated standard normal random field can be generated from the matrix L, as illustrated below:

$$G_i = \sum_{j=1}^{i} L_{ij} Z_i, \quad i = 1,2,3, \dots, n \quad (6)$$

5. Finally, the variance and mean of the parameter are reintroduced to the correlated standard normal random field, ensuring that the generated random field reflects the desired statistical properties.

$$X_i = \mu_x(x_i) + \sigma_x(x_i) G_i \quad (7)$$

The random field representing the spatial variability of the effective stress friction angle is generated, taking into account the aforementioned factors. To provide an illustration, Figure 5 depicts the distribution of effective stress friction angle as a function of depth for SOF values of 3m and 100m. The selection of observation at 3m and 100m was purposefully made to enhance the visual perceptibility of differences.

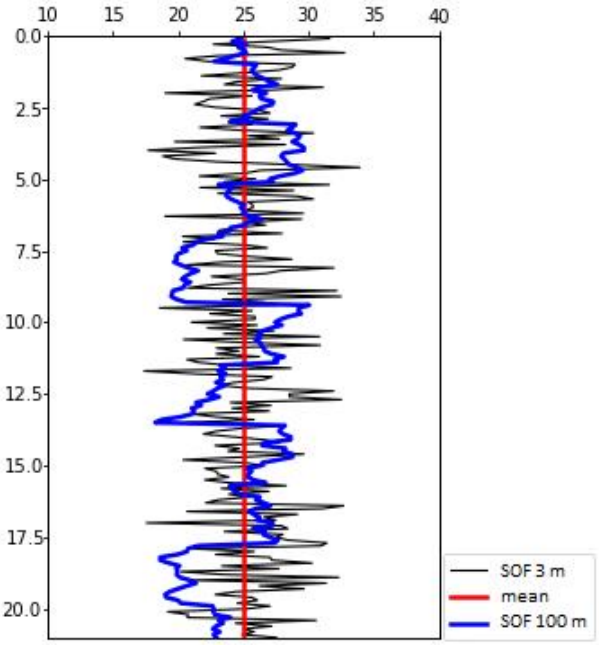

Figure 5. An example showcasing the effective stress friction angle's spatial variability simulated by using random field modeling techniques.

2.4. Monte Carlo Simulation

At its core, M-C simulation relies on the generation of random solutions or samples to provide insights into the behavior of complex systems. In statistics a common challenge is to estimate random quantities using deterministic methods. However, M-C methods offer a solution by employing random inputs to generate estimates of deterministic outputs [27]. The outputs of these random samples are then subjected to rigorous statistical calculations, enabling to extract meaningful insights and draw informed conclusions. By generating a sufficient number of random samples, one can obtain a comprehensive view of the potential outputs, allowing to accurately identify and analyze the outcomes of various random scenarios. Increasing the number of iterations leads to more precise results, yet this improvement comes at the cost of increased computational time, which grows logarithmically as the number of iterations increases. For this study, a total of 300 iterations were conducted for each analysis.

The random field generated, resembling the one shown in Figure 5, can be utilized in the finite element model of the drilled shaft wall as depicted in Figure 2.The code snippet for assignment of prestresses for anchors and creation of the random field is illustrated in Figure 6. This mapping process is repeated for 300 times, corresponding to the number of Monte Carlo simulations. As a result, the distributions of maximum bending moment and lateral wall deflection are obtained in probabilistic terms. This approach allows for the assessment of the potential range of outcomes and provides a probabilistic characterization of the behavior of the excavation system.

```
while data < iterasyon:
    g_i.gotosoil()
    dataongerme = []
    for l in range(len(g_i.NodeToNodeAnchors)):
        choices = ['Kil', 'Kum']
        weights = [0.85, 0.15]
        rnd = np.random.choice(choices, p=weights)
        if rnd == 'Kil':
            ongermekuvvet = 400
        else:
            choices2 = [70, 80, 90, 100, 110, 120, 130, 140, 150, 160, 170, 180, 190, 200]
            rnd2 = np.random.choice(choices2)
            ongermekuvvet = rnd2
        dataongerme.append(ongermekuvvet)
    print(dataongerme)
    a = np.random.uniform(0, 1, 500)
    b = np.random.choice(a, 49)
    for i in range(19):
        q = (cos(2*pi*b[i])*sqrt(-2*log(1-b[i+1])))
        c = (sin(2*pi*b[i+1])*sqrt(-2*log(1-b[i+2])))
        Z.append(q)
        Z.append(c)
        Z = Z[:21]

    G = np.zeros(21)  # Array to store G1 to G21

    for i in range(21):
        G[i] = np.sum(L[i, :i+1] * Z[:i+1])
    X = np.zeros(21)
    for i in range(21):
        X[i] = G[i]*3.25+25
```

Figure 6. Part of the Codes for Assigning Pre-stress for Anchors and Creating Random Field

In the FEM MC simulations, the occurrence of system failure is defined as exceeding either the structural capacity of drilled shafts, the prescribed limits of lateral displacement in the wall, or encountering slope stability issues. The failure in FEM is represented by a straightforward equation as provided below:

$$p = \begin{cases} -1, \ if\ plastic\ analysis\ fail & (\mathrm{M_{stage}} \neq 1) \\ 1, \ if\ plastic\ analysis\ succesfull & (\mathrm{M_{stage}} = 1) \end{cases} \quad (8)$$

Equation 8 introduces the variable "p" which is a function of the failure mechanism. To comprehensively define the failure mechanism, an additional failure mode is integrated into the analysis. This particular failure mode pertains to the prescribed limits of lateral displacement in drilled shafts. By considering this additional factor, a more complete understanding of the failure mechanism can be achieved.

According to [28], issues arise when the ratio of lateral displacement to excavation depth surpasses 0.3%. Similarly, when fine-grained soils are employed for constructing horizontally supported walls using soil nails, the Federal Highway Administration (FHWA) Design Guideline [29] recommends maintaining a lateral displacement to excavation depth ratio of 1/333. Considering these field experiences and design guidelines, an equilibrium function limiting lateral displacement was defined in FEM analyses through Equation 9:

$$p = \begin{cases} -1, & \delta_{\mathrm{ymax}} \geq 0.003\ \mathrm{H} \\ 1, & \delta_{\mathrm{ymax}} < 0.003\ \mathrm{H} \end{cases} \quad (9)$$

3. RESULTS

Expanding on the knowledge acquired from the previous sections, two variations of FEM analyses were performed, differing in the SOF for the random field of effective stress friction angle. One variant had a SOF set at 3 meters, while the other had a SOF of 21 meters. In both cases, the effective cohesion was modeled by Sorensen and Okkels' [23] formulation, which relates it to the undrained shear strength. The variable values were derived from a lognormally distributed random variable with a mean of 200 kPa and a coefficient of variation (COV) of 23%. The prestressing force of anchors was randomly determined based on the anchor's root location being in either clay or sand. This was achieved by using a fixed value of 400 kN or a uniform distribution ranging from 70 kN to 200 kN, with respective weights of 85% and 15%.

Figure 7 displays the histograms of the simulated effective stress friction angle for the two SOF values. Random fields were generated for the effective stress friction angles, and for both studies with SOF of 3 m and 21 m, the mean value of 25° with a COV of 13% was targeted. Upon examination, it is observed that there is no substantial difference in the mean and COV values between the two SOF scenarios, which is in line with the expected outcome. This indicates that the choice of SOF does not significantly impact the mean and variability of the simulated effective stress friction angle, as expected.

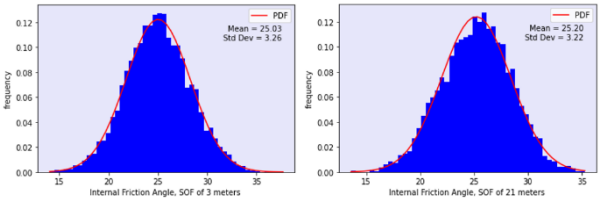

Figure 7. (a) Internal Friction Angle, SOF of 3 meters (b) Internal Friction Angle, SOF of 21 meters

Table 5 is compiled from a total of 6300 samples of effective stress friction angles, as there are 300 iterations, and 21 values of effective stress friction angles per iteration.

Table 5. Properties of Simulated Effective Stress Friction Angles for Different SOF

Effective Stress Friction Angle	Range in 300 iterations	Range of Standard Deviation per Iteration
Scale of Fluctuation of 3 meters	14.04-37.7	2.05-4.27
Scale of Fluctuation of 21 meters	13.57-35.28	1.90-4.90

The main focus of the study was to investigate the influence of spatial variability in the effective stress friction angle on the anticipated maximum lateral wall deflection and bending moment. Figure 8 illustrates the distribution of estimated maximum lateral wall deflections for two distinct spatial variability values: 3 meters and 21 meters. In Figure 8, it can be observed that when the SOF is increased from 3 meters to 21 meters, the mean value of the maximum lateral wall deflection experiences only a slight increase, from 3.39 cm to 3.45

cm. However, the more significant finding is the considerable increase in the standard deviation, which rises from 0.72 to 1.24. This indicates a much higher degree of variability and dispersion in the maximum lateral wall deflection values as the SOF increases.

Similar observations can be made for the maximum bending moment, as depicted in Figure 9. When comparing the spatial variability values of 3 meters and 21 meters, the average maximum bending moment shows only a slight increase. However, a notable 30% surge is observed in the standard deviation as the SOF changes from 3 meters to 21 meters. This indicates a significant increase in the variability and dispersion of the maximum bending moment values with the larger but a less realistic SOF.

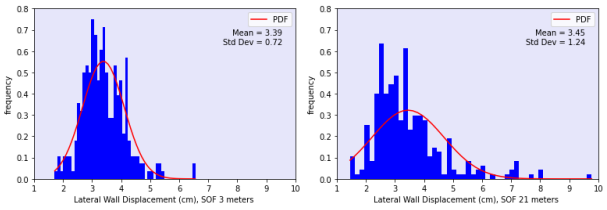

Figure 8. (a) Lateral Wall Displacements for SOF=3m, (b) Lateral Wall Displacements for SOF=21m

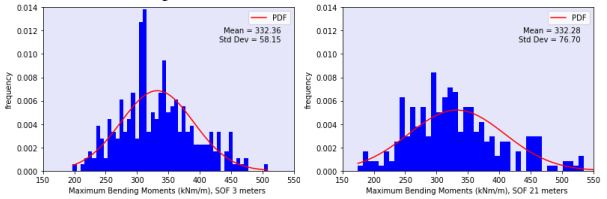

Figure 9. (a) Maximum Bending Moments for SOF=3m, (b) Maximum Bending Moments for SOF=21m

Table 6 presents the range of lateral wall displacements and maximum bending moments. As expected, the range for both the lateral displacements and the maximum bending moments increased significantly with higher SOF.

The overestimation ratio (OR) is calculated by Equation 10:

$$OR(\%) = \frac{Number\ of\ iterations\ which\ exceeds\ 0.003H\ limit}{Total\ number\ of\ iterations} \quad (10)$$

The substantial increase in standard deviations leads also to notable larger failure rates or probabilities of failure. Table 7 highlights these changes, demonstrating that the failure rate has almost doubled, rising from 9 out of 300 to 16 out of 300, as the SOF increased from 3 m to 21 m.

Table 7. Failure Rates as a Function of SOF

	SOF of 3 meters	**SOF of 21 meters**
Number of Iterations	300	300
Number of Failures	9	16
Displacement Exceeding % 0,3H	2	12
Probability of Failure (%)	3.0	5.3

The obtained results are consistent with the findings of Sert et al.[12], Fenton and Griffiths [30], and Luo et al. [13] who suggests that a smaller scale of fluctuation results yields a smaller variation of the response, i.e., the lateral wall deflection and the maximum bending moment for the case herein. It is important to note that the scenario herein with a much higher SOF of 21 meters can be considered as a case where spatial variability is not considered or simply neglected, resembling a spatially constant condition. Thus, neglecting or overlooking the spatial variability can lead to an overestimation of the maximum lateral wall deflection or bending moment, and more importantly the probability of failure.

4. CONCLUSION

This study involved the analysis of a case history where a deep excavation was supported by pre-stressed anchors. The random field theory was employed to examine the variation of internal friction angle and its influence on both lateral wall displacement and the maximum bending moment. Two different SOFs were considered, 3 meters and 21 meters. 300 FEM analyses were performed using Python 3 in PLAXIS 2D program for a comparative evaluation of results. It is important to emphasize that there is a lack of sufficient research exploring how different SOF values affect drained soil parameters in clay and their impact on the performance of excavation support systems. Additionally, only a limited number of studies have utilized verified modeling and real deformation measurements.

Table 6. Range of Lateral Wall Displacements and Maximum Bending Moments

	Range of Lateral Wall Displacement (cm)	**Range of Maximum Bending Moments (kNm/m)**	**Overestimation Ratio at 300 Iterations (%)**
Scale of Fluctuation of 3 meters	1.71-6.55	197.43-508.45	0.67
Scale of Fluctuation of 21 meters	1.45-9.77	174.56-593.66	4.0

The application of random field theory yielded mean values that exhibited proximity to those obtained from the deterministic results. However, when a SOF of 21 meters were used, higher values of coefficient of variation were obtained compared to those with smaller SOF. Despite the close similarity observed in the mean values of lateral wall displacements and maximum bending moments, the results obtained for the larger SOF exhibits a higher degree of dispersion, indicating a wider spread in the data. Consequently, although there is only a slight increase in the mean wall displacement with larger SOF values, a significant increase in the percentage of simulations exceeding the 0.003H displacement threshold was also observed. Therefore, it was clearly observed that an accurate selection of the SOF is an important consideration in risk analyses.

Based on the foregoing results, a careful consideration should be given to choosing an appropriate SOF that aligns with the objectives and requirements of the study. It can be concluded that the application of random field theory with an overestimated SOF may pose challenges to engineering decision-making, owing to the considerable data dispersion observed for lateral wall displacement and maximum bending moment.

AUTHORS' CONTRIBUTIONS

Dursun Enes KORKUT: Conducted a literature review, modeled the design in FEM, conducted the analyses and wrote the article.

Sami Oğuzhan AKBAŞ: Conducted a literature review, verified the analyses results' and wrote the article.

DECLARATION OF ETHICAL STANDARDS

The author(s) of this article declare that the materials and methods used in this study do not require ethical committee permission and/or legal-special permission.

REFERENCES

[1] Phoon KK and Kulhawy FH, "Characterization of geotechnical variability", ***Canadian Geotechnical Journal***, 36(4), 612-624, (1999a).

[2] Uzielli M., Lacasse S., Nadim F and Phoon KK, "Soil variability analysis for geotechnical practice. ***Characterisation and engineering properties of natural soils***", 3(4), 1653-1752, (2007).

[3] Schweiger HF and Peschl GM, "Reliability analysis in geotechnics with the random set finite element method", ***Computers and Geotechnics***, 32, 422-435, (2005).

[4] Lacasse S and Nadim F., "Risk and reliability in geotechnical engineering", ***St. Louis***, 1172-1192, (1998).

[5] Yu X., Cheng J., Cao C., Li E., and Feng J., "Probabilistic analysis of tunnel liner performance using random field theory." ***Advances in Civil Engineering***, (2019).

[6] Zhang S., Li Y., Li J., and Liu L., "Reliability analysis of layered soil slopes considering different spatial autocorrelation structures." ***Applied Sciences***, 10(11), 4029, (2020).

[7] Chen L., Zhang W., Chen F., Gu D., Wang L., and Wang, Z., "Probabilistic assessment of slope failure considering anisotropic spatial variability of soil properties." ***Geoscience Frontiers***, 13(3), 101371, (2022).

[8] Pană P., "Implementation of spatial variability in PLAXIS.", ***Master of Science in Applied Earth Sciences, Delft University of Technology***, (2022).

[9] Goldsworthy JS, Jaksa MB, Kaggwa WS, Fenton GA, Griffiths DV, and Poulos HG, "Reliability of site investigations using different reduction techniques for foundation design.", ***In 9th International conference on structural safety and reliability***, pp. 901-908, (2005).

[10] Wu G., Zhao H., Zhao M., and Zhu Z, "Stochastic analysis of dual tunnels in spatially random soil." ***Computers and Geotechnics***, 129, 103861 (2021) .

[11] Zhu H., Zhang L.M. " Characterizing geotechnical anisotropic spatial variations using random field theory", ***Canadian Geotechnical Journal***, 50(7), 723-734, (2013).

[12] Sert S., Luo Z., Xiao J., Gong W and Juang CH, "Probabilistic analysis of responses of cantilever wall-supported excavations in sands considering vertical spatial variability", ***Computers and Geotechnics***, 75, 182-191, (2016) .

[13] Luo N and Bathurst RJ, "Probabilistic analysis of reinforced slopes using RFEM and considering spatial variability of frictional soil properties due to compaction", ***Georisk: Assessment and Management of Risk for Engineered Systems and Geohazards***, 12(2), 87-108, (2018).

[14] Nguyen TS and Likitlersuang S., "Influence of the spatial variability of soil shear strength on deep excavation: A case study of a Bangkok underground MRT station", ***International Journal of Geomechanics***, 21(2), 04020248, (2021).

[15] Python Software Foundation. Python Language Reference, version 3.10.4. Available at http://www.python.org

[16] Çalışan O., "Ankara Kilinde Yapılan 20 m Derinliğinde Bir Kazının Geri Analizi", ***Prof. İsmet Ordemir'i Anma Toplantısı ve 5. Odtü Geoteknik Mühendisliği Sempozyumu, Ankara : METU, İnşaat Mühendisliği Bölümü***, 1-12, (2009).

[17] PLAXIS 2D (Software). (2017). PLAXIS BV. Delft, The Netherlands: P.O. Box 572, 2600 AN.

[18] Brinkgrave RBJ, "Course notes: international course for experienced Plaxis users(English)", ***The Netherlands***, (2005).

[19] Harr ME, "Reliability-based design in civil engineering", ***1984 Henry M. Shaw Lecture***. Raleigh, N.C.: Department of Civil Engineering, North Carolina State University, (1984).

[20] Bozkurt S and Akbas SO, "Finite Element-based Geotechnical Risk Analysis For Anchor–supported Deep Excavations", ***Arabian Journal of Geosciences***, (2023).

[21] Phoon KK and Ching J., "Risk and Reliability In Geotechnical Engineering", ***CRC Press Taylor ve Francis Group***, (2015).

[22] Akbas SO and Kulhawy FH, "Characterization and estimation of geotechnical variability in Ankara Clay: A case history", ***Geotechnical and Geological Engineering***, 28(5), 619-631, (2010).

[23] Sorensen KK and Okkels N., "Proceedings of the 18th international conference on soil mechanics and geotechnical engineering. Correlation between drained

shear strength and plasticity index of undisturbed overconsolidated clays", Paris, 423-428, (2013).

[24] Akademi Etüt Proje, "***DHMİ Esenboğa Havalimanı Jeolojik ve Jeoteknik Raporu***", Ankara, (2014).

[25] Vanmarcke E., "Random fields: analysis and synthesis", ***World scientific***, (2010).

[26] Fenton AG, "Data Analysis/Geostatistics", in Probabilistic Methods in Geotechnical Engineering, ***Fenton AG. Ed.***, GeoLogan'97 Logan, Utah, USA, 14-38, (1997).

[27] Johansen AM, "Monte Carlo Methods" in International encyclopedia of education, ***Elsevier Ltd.***, (2010).

[28] Long M., "Database for Retaining Wall and Ground Movements due to Deep Excavations", ***Journal of Geotechnical and Geoenviromental Engineering***, mar; 127(3): 203-224, (2001).

[29] Lazarte CA, Robinson H., Gomez JE, Baxter A., Cadden A., Berg R., "Soil Nail Walls Reference Manuel", ***U.S.: U.S. Department of Transportation Federal Highway Administration***, (2015).

[30] Fenton, GA and Griffiths, DV., "Three-Dimensional Probabilistic Foundation Settlement." ***Journal of Geotechnical and Geoenvironmental Engineering***, 131(2), 232–239. (2005).